Int J Thermophys (2013) 34:851–864
DOI 10.1007/s10765-012-1169-1

Apparent Thermal Properties of Phase-Change Materials: An Analysis Using Differential Scanning Calorimetry and Impulse Method

Zbyšek Pavlík · Anton Trník · Ján Ondruška · Martin Keppert · Milena Pavlíková · Petra Volfová · Viktor Kaulich · Robert Černý

Received: 6 October 2011 / Accepted: 6 February 2012 / Published online: 18 February 2012

Abstract Thermal properties of newly developed plaster based on hydrated lime, metakaolin, and paraffinic wax enclosed in polymer micro-capsules are studied in the article. At first, differential scanning calorimetry (DSC) is applied on Micronal PCM capsules for determination of the temperature interval of thawing and solidification. Then, the initial temperature of the phase change and specific heat capacity of the plaster are measured by DSC. The thermal conductivity and thermal diffusivity are determined by an impulse method. For comparative reasons, the properties of lime-based plaster without PCM are studied as well. The obtained results demonstrate the enhanced heat storage capacity of the studied material that can be used for application in lightweight building envelope systems.

Keywords Lime plaster · Phase-change materials · Specific heat capacity · Thermal conductivity

1 Introduction

The thermal comfort of buildings' occupants depends on the physical properties of applied building materials, on the exposure of buildings flanks to sun radiation and harmful climate conditions, and the mode of heating and ventilation. Especially the energy consumption on heating of buildings represents a serious problem for a number

Z. Pavlík (✉) · A. Trník · M. Keppert · M. Pavlíková · P. Volfová · V. Kaulich · R. Černý
Department of Materials Engineering and Chemistry, Faculty of Civil Engineering, Czech Technical University in Prague, Thákurova 7, 166 29 Prague 6, Czech Republic
e-mail: pavlikz@fsv.cvut.cz

A. Trník · J. Ondruška
Department of Physics, Faculty of Natural Sciences, Constantine the Philosopher University, Tr. A. Hlinku 1, 949 74 Nitra, Slovakia

of the developing as well as advanced countries having a cold climate. On this account, scientists all over the world are in search of new and renewable energy sources that will provide a sufficient amount of energy and reduce the CO_2 emissions from the combustion of fossil fuels [1,2].

For thermal energy storage, the use of phase-change materials (PCMs) has received great interest in recent years [3–5]. Application of latent heat storage building envelope systems using PCMs represents an effective way of storing the thermal energy and has the advantages of a high energy storage density and the isothermal nature of the storage process [6]. Since energy storage in walls, ceilings, floors, and other building components may be effectively enhanced and moderated by suitable PCMs [7–10], it is possible to maintain the internal temperature of buildings closer to the desired comfort temperature for a longer period, without any other additional energy for cooling and heating. This performance of building structures composed of PCMs is beneficial especially in extremely hot and cold climates, where the energy consumption for maintaining the comfort of internal conditions of buildings varies significantly during the day and the night.

Theoretically, latent heat storage can be accomplished through solid–liquid, liquid–gas, solid–gas, and solid–solid phase transitions [11]. However, from a practical point of view, taking into account the real conditions of building structures, only the PCMs working on a phase change from the solid-to-liquid or solid-to-solid phases can be used. Although the solid–gas and liquid–gas transitions have a higher latent heat of fusion, their large volume changes for a phase transition are associated with containment problems and rule out their potential utility in thermal storage systems [6]. The solid–solid phase transition is characterized by heat storage within the materials transformation from one crystalline structure to another. This transition usually has a smaller latent heat and volume change than for a solid–liquid transition, whereas its main advantages represent less rigorous container requirements and better design flexibility [11]. In practice, usually the solid–liquid transition is utilized and it has proved to be economically attractive for effective thermal energy storage systems. In the case of the application of PCMs operating on the phase change between a solid and liquid, encapsulation of the PCM is necessary to avoid leakage of a liquid PCM [12]. In addition, the PCM containment must fulfill the requirements of strength, flexibility, corrosion resistance, and thermal stability. The PCM encapsulation acts as a barrier against a harmful interaction with the environment and must provide sufficient surface area for heat transfer to the encapsulated PCM [12,13]. PCM capsules are usually classified into macro- and micro-capsules, whereas macro-capsules are considered to be the most conventional PCM capsules and many papers have reported various shell materials, such as metal and polymers, and various shapes such as spherical and cylindrical [12,14–17]. Micro-encapsulation of PCMs has in comparison with macro-capsules many benefits, such as reduction of the reactivity of PCMs with the ambient environment, and increase of the heat transfer area. It also enables the core material to withstand frequent changes in the volume of the storage materials during a phase change [12,18–20].

There are a large number of PCMs (organic, inorganic, and eutectic), which can be identified as PCMs from the point of view of the melting temperature and latent heat of fusion [6]. For application in the regulation of the heat storage of building

structures, such materials must be used that exhibit the phase transition in the temperature range corresponding to the thermal climatic loading of buildings. According to the literature, paraffinic wax is the most often used commercial organic heat storage PCM [21], having melting temperatures in the range of 23 °C to 67 °C [12,22], which is optimal for control of the interior climate of buildings.

Since the benefit of PCMs for the indoor environmental quality of buildings has been already demonstrated, there is a need to develop and test new building materials with PCMs and design them for specific applications in the building industry. Probably the lowest heat storage capacity is exhibited by lightweight building envelopes composed of wooden load-bearing frames, thermal insulation, a vapor-proof layer, and gypsum wallboards. On that account, a newly developed plaster that should enhance the heat storage capacity of lightweight building envelopes is studied in this article. This material is based on hydrated lime as the major binder and the durability of this material is enhanced by the addition of metakaolin. The paraffinic wax enclosed in polymer micro-capsules is added to the dry mixture. For this studied material, the measurement of basic physical, heat transport, and storage parameters is done to evaluate the positive effect of the addition of a PCM on the heat storage capacity within the specific temperature changes.

2 Studied Material

Lime plaster modified with Micronal PCM and pozzolana based on calcined kaoline mixed with milled mudstone was the analyzed material. This material should find application in moderation of the heat storage in lightweight building envelopes. For an evaluation of the PCM addition contribution to the heat storage capacity of the developed material, the reference plaster without PCM addition was studied as well.

The applied pozzolana material was prepared using calcination of raw kaoline in a rotational kiln at a temperature close to 750 °C, and consequent milling in a rotational silo. To this "metakaolin" was then added milled mudstone, and the mixture was homogenized. The final material was very fine, having a specific surface area of $14.56\,\mathrm{m^2 \cdot g^{-1}}$ and D_{50} of $4.09\,\mu\mathrm{m}$ [23]. The chemical composition of used pozzolana measured by X-ray fluorescence analysis is presented in Table 1.

Micronal PCM was a fine powder material based on paraffinic wax encapsulated in polymer spherical micro-capsules, a product of BASF.

Lime hydrate was produced by the lime kiln Čertovy schody, Inc., Czech Republic, whereas the silica sand was from a sand-pit, Hlavačov, Czech Republic. The water/dry substances (w/d) ratio was slightly modified to keep the workability of fresh mixtures on the same level. Compositions of the studied plasters are given in Table 2.

The samples were cast from the fresh mixture of studied plasters into molds having dimensions of $70/70/70\,\mathrm{mm^3}$, $50/50/50\,\mathrm{mm^3}$, and $20/20/5\,\mathrm{mm^3}$.

3 Experimental

Within the experimental analysis of studied materials, the measurement of basic physical properties and heat transport and storage properties was done to evaluate the effect

Table 1 Chemical composition of used pozzolana

Chemical substance	Amount (mass%)
SiO_2	52.4
Al_2O_3	41.3
Fe_2O_3	1.19
TiO_2	1.77
CaO	0.14
MgO	0.15
K_2O	0.79
Na_2O	<0.01
P_2O_5	0.07
ZrO_2	0.03
V_2O_5	0.05
F	<0.01
Cr_2O_3	0.03
SO_3	0.10

Table 2 Composition of studied plasters

Plaster	$w/d(-)$	Lime hydrate (kg)	Pozzolana (kg)	Sand 0–4 mm (kg)	Micronal PCM (kg)
Reference	0.21	1.5	1.0	7.5	0.0
With PCM	0.24	1.5	1.0	7.5	1.5

of PCM addition on the plasters' performance. All the experiments were realized in an air-conditioned laboratory at a constant temperature of 23 °C ± 1 °C and a relative humidity of 30 % ± 5 %.

3.1 Determination of Basic Material Properties

At first, the powder density and particle size distribution of Micronal PCM were measured. The powder density was measured gravimetrically, weighing the known mass of material in the measuring cylinder. The particle size distribution was measured, based on the laser diffraction principle, using the device Analysette 22 Micro Tec plus.

For the researched plasters, measurements of the bulk density, matrix density, and total open porosity were performed. The experiments were carried out on four cubic samples, each with a side dimension of 50 mm. The relative expanded uncertainty of the applied testing method was 5 % and was mainly due to the material inhomogeneity. The bulk density was determined from direct measurements of sample sizes (using a digital length meter) and its dry mass. The matrix density was accessed by helium pycnometry using the Pycnomatic ATC apparatus. It applies the well-known technique of helium displacement to measure the real density of solid substances [24]. Since helium is an inert element and has a very small atom, it can penetrate even extremely

narrow pores in a solid. Within the application of the Pycnomatic ATC, a well dried sample of the studied material is weighed and placed in a calibrated reference chamber of known volume. Helium is first loaded at a known pressure in a calibrated reference chamber and then expanded into the sample chamber. Once the pressure is stabilized, experimental data are collected and the material volume is accessed. The uncertainty of the gas volume measurement using this device is 0.01 % of the measured value, whereas the uncertainty of the used analytical balances is 0.0001 g [25]. On the basis of the bulk density and matrix density measurements, the total open porosity ψ (−) was calculated using

$$\psi = 100\,(1 - \rho_v/\rho_{\mathrm{mat}})\,, \tag{1}$$

where $\rho_{\mathrm{mat}}(\mathrm{kg}\cdot\mathrm{m}^{-3})$ is the matrix density and $\rho_v(\mathrm{kg}\cdot\mathrm{m}^{-3})$ is the bulk density.

For a detailed analysis of the materials' structure, the measurement of the pore size distribution was done by mercury intrusion porosimetry (MIP) using the Pascal 140 and 440 (Thermo) apparatus. The assumed contact angle of mercury and the sample was 130°, the surface tension of mercury was $480\,\mathrm{mN}\cdot\mathrm{m}^{-1}$, and the density of mercury was $13\,534\,\mathrm{kg}\cdot\mathrm{m}^{-3}$.

The particle size distribution was measured also for the dry mixtures of both plasters, using the laser diffraction method.

3.2 DSC Analysis

Differential scanning calorimetry (DSC) analysis was performed using the DSC 822e (Mettler Toledo) apparatus with the Julabo FT 900 cooling device. The measurements were performed for the Micronal PCM, the reference plaster, and plaster modified by PCM addition. For the measurement, the particular samples were first crushed in a laboratory mill. The following temperature regime was applied: 5 min of the isothermal regime; cooling at $10\,^{\circ}\mathrm{C}\cdot\mathrm{min}^{-1}$ from 40 °C to 10 °C; 5 min of the isothermal regime; heating at $10\,^{\circ}\mathrm{C}\cdot\mathrm{min}^{-1}$ from −10 °C to 40 °C; and 5 min of the isothermal regime. On the basis of DSC analysis, the temperature of the phase transition was accessed as well as the temperature-dependent specific heat capacity.

3.3 Measurement of Thermal Conductivity and Thermal Diffusivity

The thermal conductivity and thermal diffusivity were measured using the ISOMET 2104 (Applied Precision, Ltd.) commercial device. ISOMET 2104 is a multifunctional instrument for measuring thermal properties of materials. It is equipped with various types of optional probes: needle probes are for porous, fibrous, or soft materials, and surface probes are suitable for hard materials. The measurement is based on an analysis of the temperature response of the analyzed material to heat flow impulses [26]. The heat flow is induced by electrical heating using a resistance heater having direct thermal contact with the surface of the sample [27,28]. The measurements in this article were done on cubic samples having side dimensions of 70 mm, whereas the surface probes were applied. The measurement uncertainty is for the thermal conductivity

interval ranging from (0.7 to 6.0) $W \cdot m^{-1} \cdot K^{-1}$ and is equal to 10 % of the measured value. The reproducibility of particular measurements is 3 % of the measured value of $+0.001\,W \cdot m^{-1} \cdot K^{-1}$.

4 Results and Discussion

Figures 1, 2, 3, 4, 5, and 6 show the particle size distribution of the studied materials measured by laser diffraction. Here, a very fine particle size distribution of Micronal PCM was observed. We can see that the highest number of particles was around 10 μm. The reference plaster exhibited a more uniform particle size distribution, whereas the

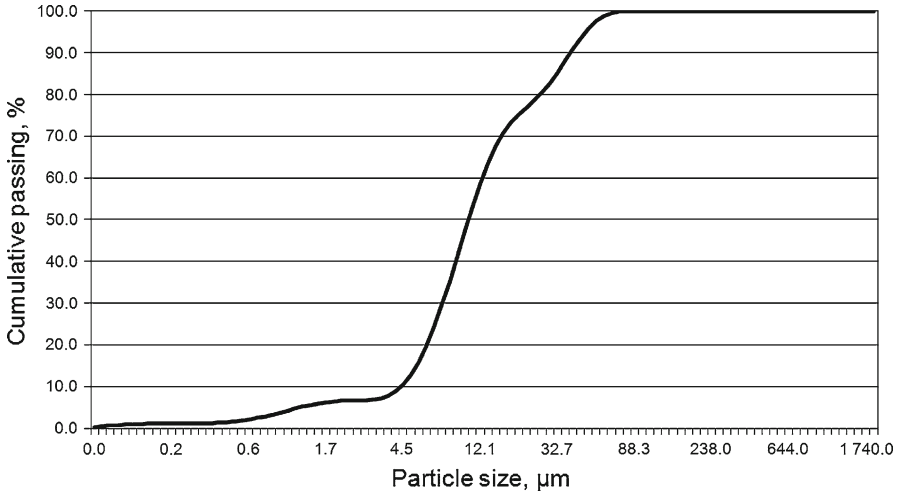

Fig. 1 Particle size distribution of Micronal PCM—cumulative curve

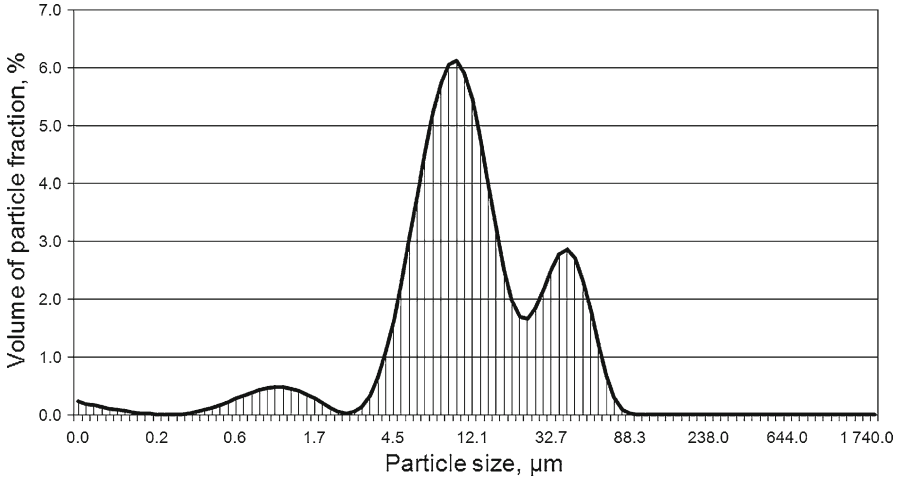

Fig. 2 Particle size distribution of Micronal PCM—distribution curve

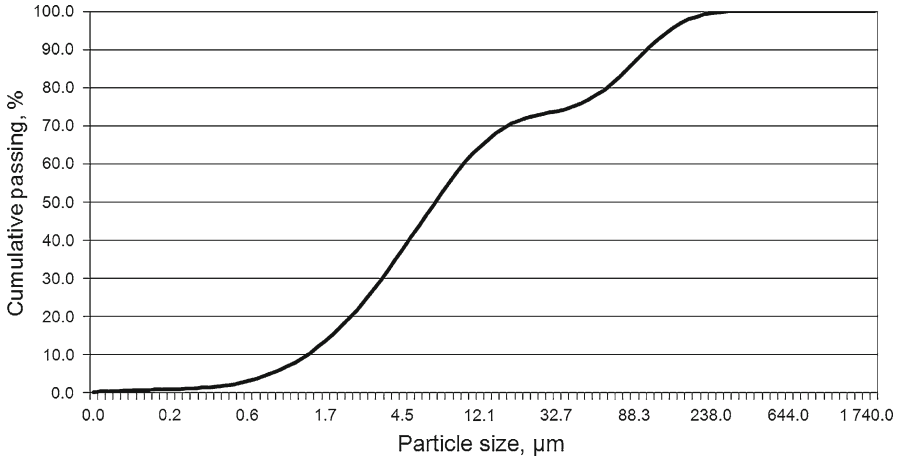

Fig. 3 Particle size distribution of the reference plaster dry mixture—cumulative curve

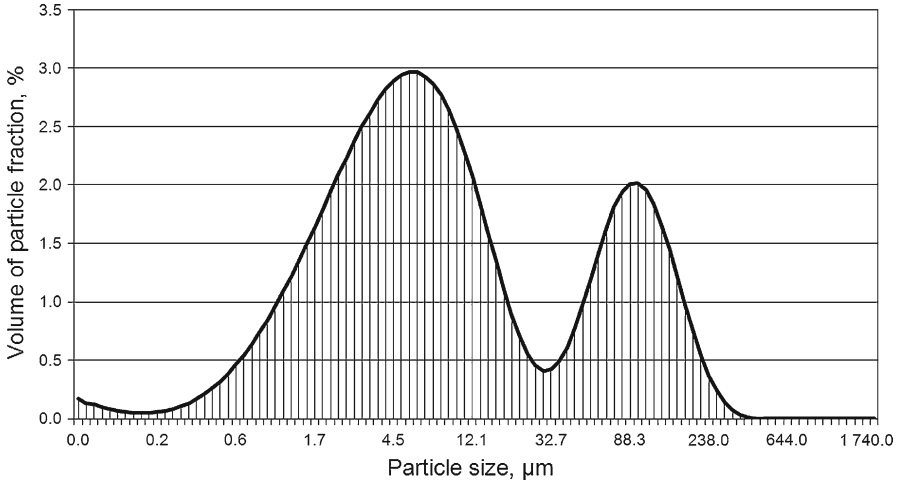

Fig. 4 Particle size distribution of the reference plaster dry mixture—distribution curve

maximum number of particles was between 5 µm and 90 µm. The particle size distribution of a plaster mixture modified by a PCM was largely affected by the Micronal PCM addition.

Basic material properties of the investigated materials are given in Table 3. We can see a very low powder density of Micronal PCM that affected the matrix density and bulk density of the plaster modified by PCM addition. The total open porosity of the modified plaster was lower in comparison with the reference plaster, which can be attributed to the capability of fine-grained PCM admixture to fill the voids in the mixture, fittingly completing the granulometry curve of the silica aggregate.

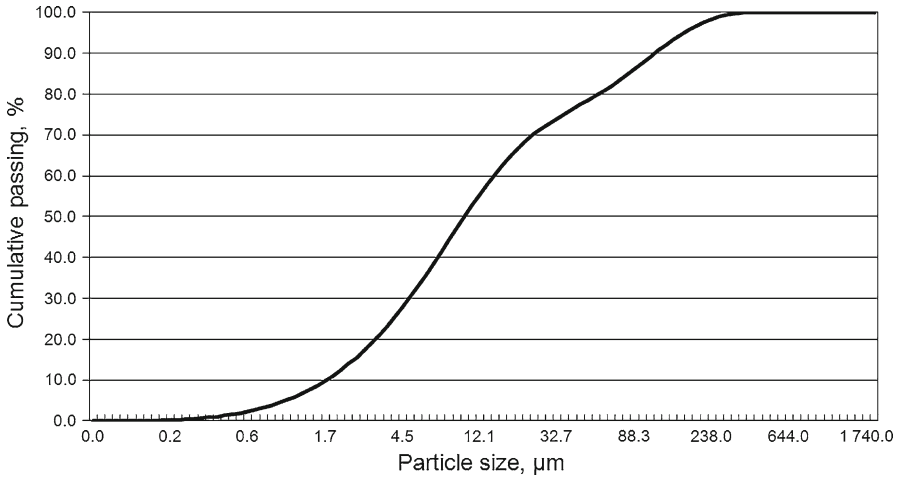

Fig. 5 Particle size distribution of the PCM-modified plaster mixture—cumulative curve

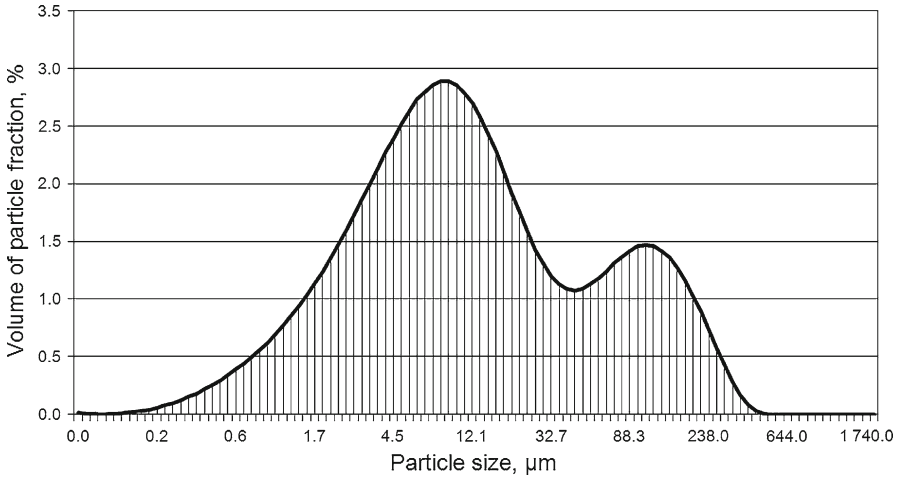

Fig. 6 Particle size distribution of the PCM-modified plaster mixture—distribution curve

Results of MIP measurements are presented in Fig. 7. The PCM-modified plaster had a higher number of bigger pores, with a peak close to 1 µm, whereas the main peak of the reference plaster was at 0.2 µm.

Figures 8, 9, 10, 11, 12, and 13 describe the data obtained within the DSC analysis. The data were graphed using the STARe SW 9.1 software that controlled also the DSC device. The temperature of the phase change of the Micronal PCM during the cooling process was 19.45 °C and 26.97 °C during heating. For the modified plaster exposed to the cooling process, we measured the temperature of the liquid–solid transition which was equal to 20.45 °C. The solid–liquid transition of modified plaster was detected at 26.27 °C. One can see that the temperatures of phase transitions for the Micronal

Table 3 Basic physical properties of studied materials

Material	Powder density ($kg \cdot m^{-3}$)	Bulk density ($kg \cdot m^{-3}$)	Matrix density ($kg \cdot m^{-3}$)	Total open porosity ($\%m^3 \cdot m^{-3}$)
Micronal PCM	359	–	–	–
Reference pl.	–	1861	2605	28.6
Pl. with PCM	–	1573	2133	26.2

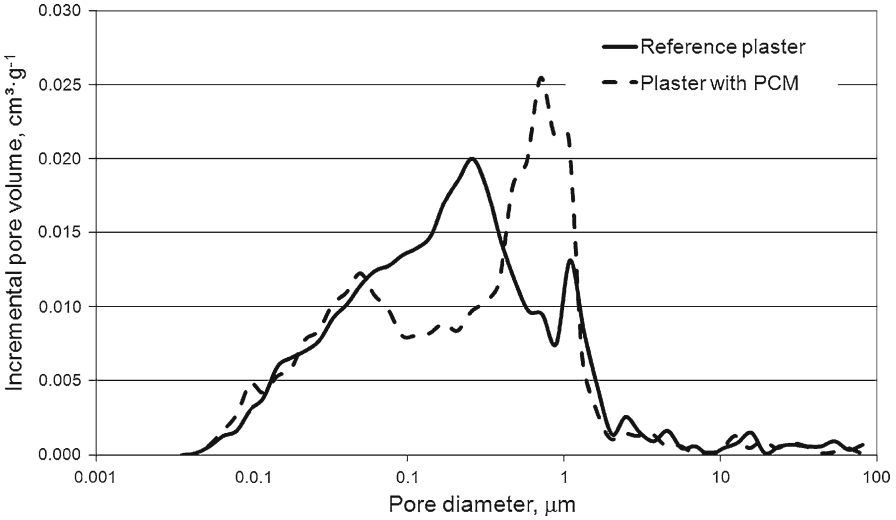

Fig. 7 Pore size distribution of studied plasters

PCM and modified plaster were more or less similar, which is beneficial for latent heat storage in the developed material.

The temperature-dependent apparent specific heat capacity of the developed and reference plaster during cooling and heating is presented in Figs. 14, 15, 16, and 17. In both temperature exposure cases, a high increase of the specific heat capacity at the temperature close to the PCM phase transition was registered for the PCM modified plaster. In comparison with the reference plaster, the newly developed plaster exhibited a higher apparent specific heat capacity over the whole studied temperature range.

In Table 4, the data obtained using the impulse method are presented. The thermal conductivity of the modified plaster was slightly higher in comparison with the reference plaster although its open porosity was somewhat lower (Table 3). This could be caused by the different topology of both plasters as indicated by the differences in their pore distributions (Fig. 7). The thermal diffusivity of the modified plaster was almost a factor of three lower as compared with the reference plaster; this was clearly a consequence of its much higher apparent specific heat capacity (Figs. 16, 17).

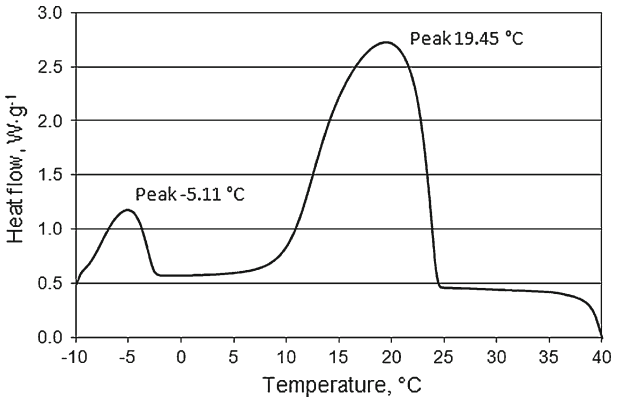

Fig. 8 Heat flow during the cooling of Micronal PCM

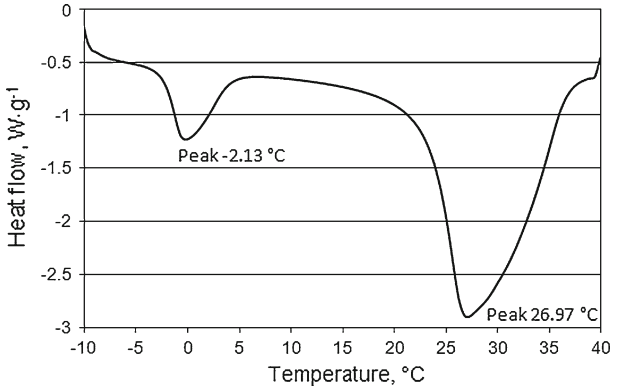

Fig. 9 Heat flow during the heating of Micronal PCM

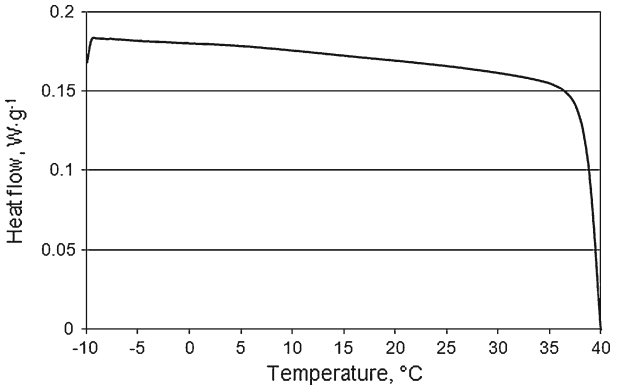

Fig. 10 Heat flow during the cooling of the reference plaster

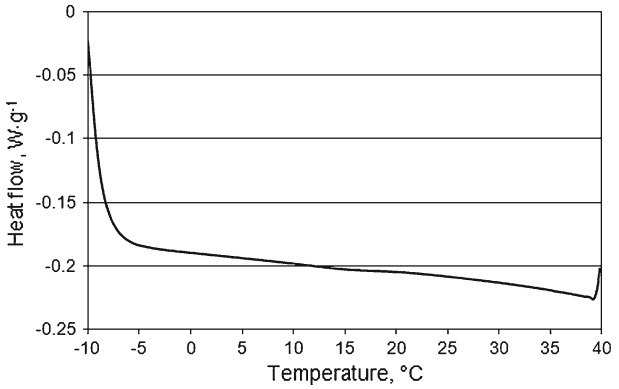

Fig. 11 Heat flow during the heating of the reference plaster

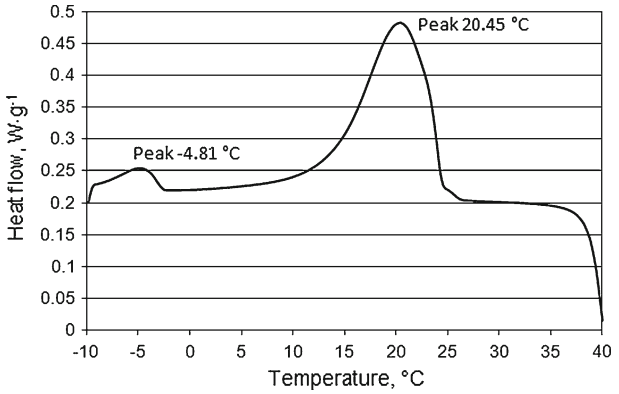

Fig. 12 Heat flow during the cooling of the plaster with PCM addition

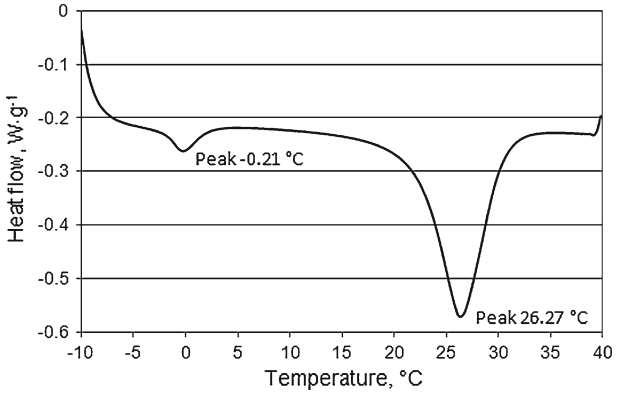

Fig. 13 Heat flow during the heating of the plaster with PCM addition

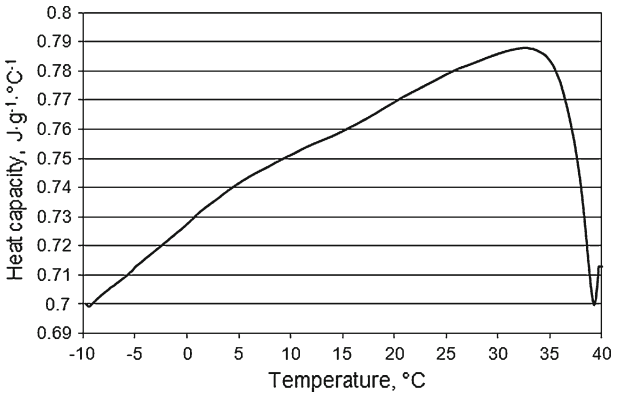

Fig. 14 Apparent specific heat capacity of the reference plaster—cooling process

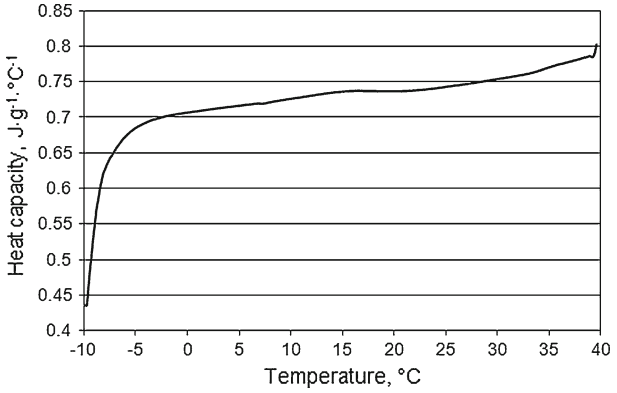

Fig. 15 Apparent specific heat capacity of the reference plaster—heating process

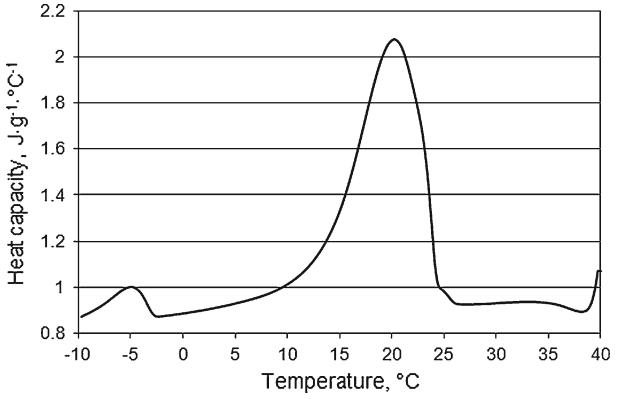

Fig. 16 Apparent specific heat capacity of the plaster with PCM addition—cooling process

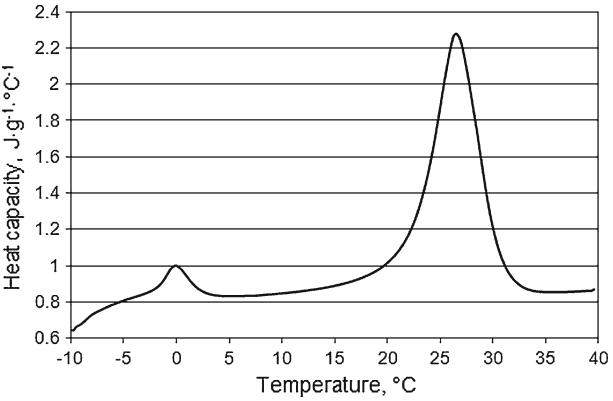

Fig. 17 Apparent specific heat capacity of the plaster with PCM addition—heating process

Table 4 Results of the impulse method

Material	Thermal conductivity ($W \cdot m^{-1} \cdot K^{-1}$)	Thermal diffusivity ($m^2 \cdot s^{-1}$)
Reference plaster	0.86	1.54×10^{-6}
Plaster with PCM	0.89	0.56×10^{-6}

5 Conclusions

The laboratory tests presented in the article revealed the positive effect of Micronal PCM incorporation on the thermal performance of a modified lime-based plaster. The phase transitions of PCM caused substantial latent heat storage as a function of the temperature exposure of the material. Thus, the application of PCM capsules with paraffinic wax led to a significant increase of the apparent specific heat capacity of the developed plaster in comparison with the reference material. This finding is very promising for the practical application of the developed plaster in lightweight building envelopes, where heat accumulation is typically very low.

Acknowledgment This research has been supported partially by the Czech Ministry of Education, Youth and Sports, under Project No. MSM 6840770031.

References

1. Z. Pavlík, R. Černý, Appl. Therm. Eng. **29**, 1941 (2008)
2. Z. Pavlík, R. Černý, Energy Build. **40**, 673 (2008)
3. Y. Zhong, Q. Guo, S. Li, J. Shi, L. Liu, Sol. Energy Mater. Sol. Cells **94**, 1011 (2010)
4. A.M. Kudhair, M.M. Farid, Energy Conserv. Manag. **45**, 263 (2004)
5. A. Sharma, V.V. Tyagi, C.R. Chen, D. Buddhi, Renew. Sustain. Energy Rev. **13**, 318 (2009)
6. S.D. Sharma, K. Sagara, Int. J. Green Energy **2**, 1 (2005)
7. M. Koschenz, B. Lehmann, Energy Build. **36**, 567 (2004)
8. T. Lee, D.W. Hawes, D. Banu, D. Feldman, Sol. Energy Mater. Sol. Cells **62**, 217 (2000)
9. M. Hadjieva, R. Stoykov, T. Filipova, Renew. Energy **19**, 111 (2000)
10. A. Pasupathy, R. Velraj, R.V. Seeniraj, Renew. Sustain. Energy Rev. **12**, 39 (2008)

11. X. Wang, E. Lu, W. Lin, T. Liu, Z. Shi, R. Tang, C. Wang, Energy Conserv. Manag. **41**, 129 (2000)
12. T. Nomura, N. Okinaka, T. Akiyama, ISIJ Int. **50**, 1229 (2010)
13. A.F. Regin, S.C. Solanki, J.S. Saini, Renew. Sustain. Energy Rev. **12**, 2438 (2008)
14. E. Assis, L. Katsman, G. Ziskind, R. Letan, Int. J. Heat Mass Transf. **50**, 1790 (2007)
15. H. Koizumi, J. Appl. Therm. Eng. **24**, 2583 (2004)
16. C. Arkar, S. Medved, Thermochim. Acta **438**, 192 (2005)
17. A.F. Regin, S.C. Solanki, J.S. Saini, Renew. Energy **31**, 2025 (2006)
18. Y.F. Fan, X.X. Zhang, X.C. Wang, J. Li, Q.B. Zhu, Thermochim. Acta **413**, 1 (2004)
19. X.L. Shan, J.P. Wang, X.X. Zhang, Thermochim. Acta **494**, 104 (2009)
20. S. Qingwen, L. Yi, X. Jianwei, J.Y. Hu, M. Yuen, Polymer **48**, 3317 (2007)
21. G.A. Lane, *Solar Heat Storage: Latent Heat Materials*, vol. 1 (CRC Press, Boca Raton, 1983)
22. A. Abhat, Sol. Energy **30**, 313 (1983)
23. Z. Pavlík, L. Fiala, M. Pavlíková, R. Černý, in *Proceedings of 12th International Conference on Durability of Building Materials and Components* (Faculdade de Engenharia da Universidade do Porto, Porto, 2011), pp. 745–752
24. M. Pavlíková, Z. Pavlík, M. Keppert, R. Černý, Constr. Build. Mater. **25**, 1205 (2011)
25. L. Fiala, M. Pavlíková, Z. Pavlík, M. Keppert, R. Pernicová, J. Mihulka, H. Benešová, R. Černý, in *Proceedings of 1st Central European Symposium on Building Physics* (Technical University of Lodz, Lodz, 2010), pp. 127–133
26. E. Mňahončáková, M. Jiřičková, Z. Pavlík, L. Fiala, P. Rovnaníková, P. Bayer, R. Černý, Int. J. Thermophys. **27**, 1228 (2006)
27. M. Jiřičková, Z. Pavlík, L. Fiala, R. Černý, Int. J. Thermophys. **27**, 1214 (2006)
28. Z. Pavlík, E. Vejmelková, L. Fiala, R. Černý, Int. J. Thermophys. **30**, 1999 (2009)